Geochemistry and petrogenesis of dyke swarms in NW Sinai, Egypt: a case of transition from compressional to extensional regimes during the late Neoproterozoic

Said A. El-Nisr[1,2], Adel A. Surour[1,3*], Asaad M. B. Moufti[1]

1- Department of Mineral resources and rocks, Faculty of Earth Sciences,King Abdulaziz University, P. O. Box 80206, Jeddah 21589, Saudi Arabia.
2- Geology Department, Faculty of Science, Alexandria University, Egypt.
3- Geology Department, Faculty of Science, Cairo University, Egypt.

* Corresponding Author: aasurour63@hotmail.com

Received: 13March 2014 / Accepted: 25 May 2014 / Published online: 05July 2014

Abstract

Dyke swarms emplacement constitutes one of the conspicuous features of the Neoproterozoic Arabian-Nubian Shield (ANS) (~950-540Ma). Based on field investigations, petrographic and geochemical characteristics the dyke swarms in NW Sinai (Egypt) comprise of mafic (dolerite-trachy-basalt-basalt), intermediate (basaltic-andesite trachy-andesite) and felsic (rhyodacite-rhyolite) varieties. Geochemically, all varieties are calc-alkaline with the exception of few mafic varieties that show weak alkaline affinity. Increasing SiO_2 is accompanied by enrichment in Na_2O, K_2O and depletion of TiO_2, FeO^t, MgO, CaO, P_2O_5, Co, Sr, Ba, Zr and Y. There is a compositional gap between the mafic, intermediate and the felsic dykes perhaps indicating more than one magma source. Although, Geochemical signatures of the investigated dykes swarms suggest that they are related to subduction processes,but according to tectonics and field relationships the studied dykes represent a post-orogenic or, at least, represent a transitional tectonic setting between Subduction and extension phases. The mafic dykes resulted from a lithospheric mantle-enriched material during a previous subduction event (> 300 Ma) by small degree of partial melting.The intermediate dykes are most probably produced by partial melting of basaltic magma that followed by fractional crystallization processes. Fractional crystallization processes are dominated during the evolution of the most evolved intermediate samples; due to consumption of pyroxene, amphibole and plagioclase. The felsic dykes most probably evolved by partial melting of a lower mafic crust which led to the formation of a rhyolitic magma. In addition, the investigated samples showed remarkable crustal contamination during their formation. The investigate dyke swarms were emplaced at a post-orogenic extensional collapse event transitional between volcanic-arc and within-plate environment during the late stages of the Late Neoproterozoic juvenile Pan-African crust of the Sinai Peninsula.

Keywords: Neoproterozoic, Dyke Swarms, Post-Orogenic, Multiple Magma Source, Sinai Peninsula.

1–Introduction

It is widely accepted that the crust of the Arabian-Nubian Shield (ANS) was generated during the Pan-African orogenic event (~950-540 Ma; Kröner, 1985) and was oneof the most voluminous events of juvenile crust formation that extends over an area of about2 millionkm^2 on both sides of the Red Sea (Bentor, 1985; Stern, 1994). Rb-Sr and U-Pb geochronological data suggest that subduction processes were ceased-600 Ma ago (Stern and Hedge, 1985; Stern, 1994; Greiling *et al*., 1994). The final stage of cratonization (600-540 Ma) was dominated by NW-trending strike-slip faults

(Najd fault system); and strong extension which was accompanied by bimodal magmatic activity and the deposition of molasses-type sediments (e.g. Stern, 1985; Jarrar *et al*., 1992; Wilde and Youssef, 2000, 2002). The post-collisional magmatism is dominated by undeformed calc-alkaline and alkaline/peralkaline granitoids, constituting ~ 80% of the basement outcrops in the northern part of the Neoproterozoic ANS, as well as the volcano-sedimentary successions including the so-called DokhanVolcanics. Dykes in the Nubian Shield of Egypt represent a transitional period from compressional subduction-related magmatism (Ragab, 1987; El Gaby *et al*., 1989; and Abdel Rahman, 1996) to extensional-related magmatism (Ressetar and Monrad, 1983; Stern *et al*., 1984 & 1988; Mohamed *et al*., 2000). However, the eruption of high-K magmas with a typical element signature records post-dating active subduction that took place synchronous with uplift, extension or strike-slip motion (Sloman, 1989). In the Eastern Desert and Sinai Peninsula, dyke rocks of basaltic to rhyolitic-composition are closely associated with granitoids and intruded under extensional conditions (Stern *et al*., 1988; Friz-Töpfer, 1991; Beyth and Peltz, 1992; El-Nisr and Moghazi, 2001).

The investigated dyke swarms are unmetamorphosed post-orogenic (591± 9 Ma) according to Stern and Manton (1987); Helba (1989) and El-Nisr (1990).The Precambrian dykes in the Sinai Peninsula are mostly post-orogenic and are confined to early Tonian-Cryogenian fracture system (Fowler *et al*., 2010). These dykes pre-date the late Edicaran (605-580 Ma) anorogenic alkaline magmatism of the so-called Katherina A-type rhyolites (Farahat and Azer, 2011; El-Baily and Hassen, 2012; Azer, 2013).Rb-Srdating gave an isochron age of 591± 9 Ma(Stern and Manton, 1987) for some basaltic-acidic dykes from WadiFeiran.Some relatively younger mafic dykes in Jordan (545±13 Ma) represent the youngest Neoproterozoic dyke suite in the ANS (Jarrar, 2001). There is an agreement that the KatherinaVolcanics are Late Precambrian which were derived from a crustal source mixed with a juvenile mantle magma (Azer, 2007). Many scientists worked on the Pan-African dyke swarms in Sinai Peninsula(Stern and Manton, 1987; Helba, 1989; El-Nisr, 1990; El-Shishtawy, 1994 and El-Sayed 2006).In the Sinai Peninsula as well as in other Egyptian localities, the Phanerozoic volcanics are widespread in age (Early Paleozoic-Mesozoic-Cenozoic) (Wassif, 1991; Perrin *et al*., 2009; Abu El-Maaty *et al*., 2011). The early Paleozoic ones are possibly coincided with the waning stage of the Pan-African orogeny (~ 550-500 Ma, Perrin *et al*., 2009).

The present study aims to discuss the problem of tectonic environment in which the investigated post-orogenic dyke swarms (591± 9Ma; Stern and Manton, 1987) were erupted. Along with this, geochemical data are used to provide constraints on the source characteristics and process(es) by which the magma was evolved. The possibility of partial melting and/or fractional crystallization processes that govern the bimodality of the investigated dyke swarms will be discussed in the light of recently investigated bimodal mafic-felsic dykes outside the ANS, such as in NE China and Southern Australia (e.g. Sun *et al*., 2013; Kromkhun *et al*., 2013, respectively).

2–Geological setting

The area under investigation is composed of gneisses; migmatites; metavolcanics; metagabbro-diorite complex; older granitoids; acid alkaline volcanics and post-orogeneic leucogranite (Fig. 1).The area was previously studied by Stern and Manton (1987); Helba, 1989;El-Nisr (1990); El-Shishtawy, 1994; El-Metwally, *et al*., 1998 and El-Sayed(2006). All metamorphic and plutonic rocks in the study area are cut by post-orogenic dykes of mafic, intermediate and felsic compositions. The investigated dyke rocks are contemporaneously,

unmetamorphosed, nearly vertical to sub-vertical not equally distributed in th study area and show sharp contacts against their host rocks and display chilled margins. Mafic dykes -the most youngest variety-are most abundant dyke rocks and intruded into the younger granitoids. Mafic dykes in the study area comprise of basalt, trachy-basalt and dolerite varieties.

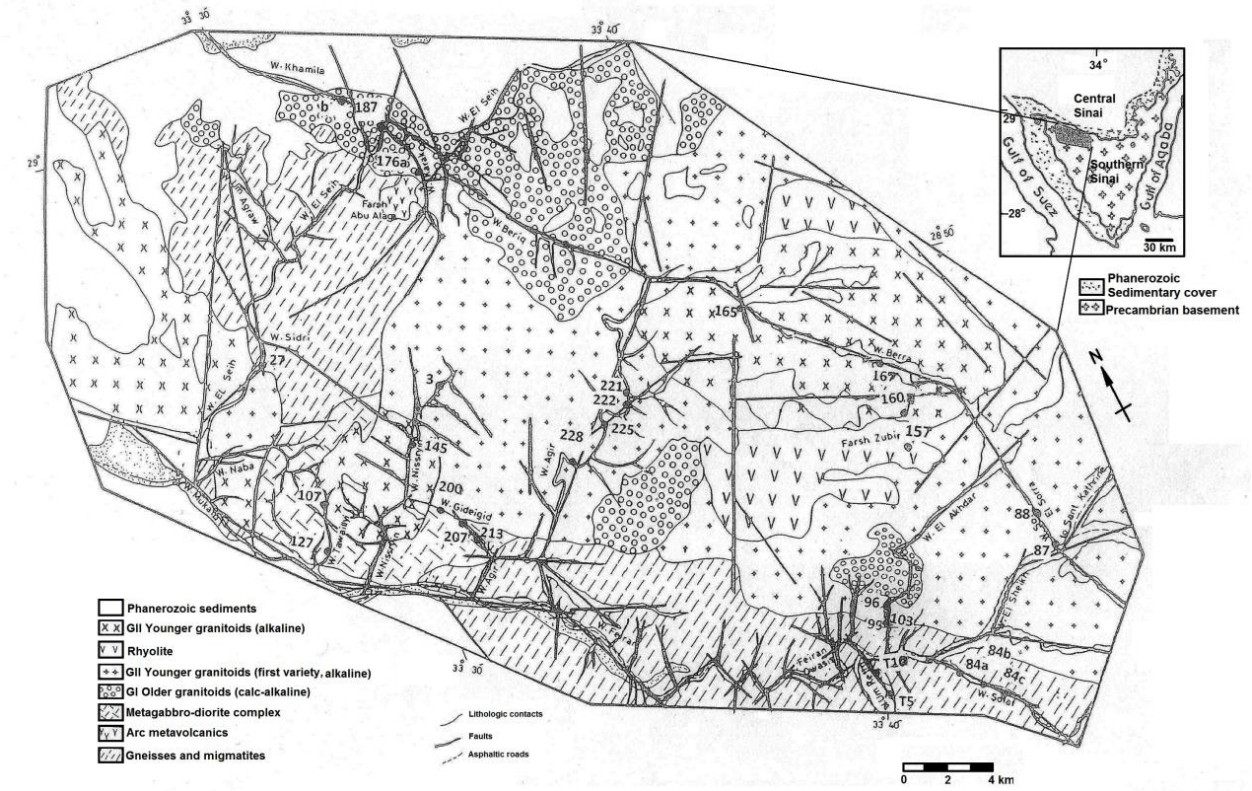

Figure 1) Simplified geologic map of the study area in the north-western Sinai basement rocks, Egypt. (modified after El-Nisr, 1990).

The mafic dykes crosscut older granitoids, post-orogenic leucogranite, while Feiran gneisses and migmatites are occasionally invaded by these dykes. The intermediate dykes are represented by basaltic-andesites and trachy-andesites that generally intruded into the younger granitoids. The trachy-andesite variety is the most dominant among the intermediate dykes. Felsic dykes comprise abundant varieties, namely granitic, rhyolitic, quartz porphyry, granopheric and aplitic varieties. These felsic dykes mainly intruded into the granitoid rocks, Feiran gneisses-migmatites and the metagabbro-diorites. The Felsic dykes (Fig. 2) form a positive relief with respect to the enclosing rock and are dissected by columnar and horizontal sets of joints. However, the intrusion of the felsic dykes in the post-orogenic leucogranite is not infrequent.

Structurally, the area under investigation (Fig. 1) is affected by the tectonic and structural elements that influenced the Arabian-Nubian Shield in general and the Sinai Peninsula in particular, from early Precambrian until the Oligocene-Miocene Red Sea rifting time. The study area is structurally controlled by two well develop trends (NE and NW).

Figure 2) An example of NW Sinai dykes: sub-parallel felsic dykes traversing the leucogranite of Wadi El-Akhdar.

The NE trend (mostly occupied by dykes) is considered as old tensional fractures that have been developed mostly by tensional forces in a NW direction. The NW trend is less developed than the NE one and is usually cut by the latter. The NW trend is dominated for faults and some joint sets; that might be originated from extensional stresses in a NE direction (Helba, 1989; El-Nisr, 1990).

3–Petrography

Many samples have been collected from the dyke swarms of different compositions (mafic, intermediate and felsic) in the area under investigation are microscopically studied.

3.1- Mafic dykes

The main mafic dykes consist of three varieties: dolerites, basalts and trachy-basalts. They are massive medium- to fine-grained, dark black or grey with greenish and reddish tints. The porphyritic nature is manifested by plagioclase phenocrysts embedded in an aphanitic groundmass in the trachy-basalts and basalts varieties. The former is the most abundant variety of mafic dykes. Microscopically, the mafic dykes consist of plagioclase feldspar, pyroxene and amphibole. Chlorite, sericite and calcite as alteration products, whereas Fe-Ti oxides, apatite and titaniteare the main accessories.

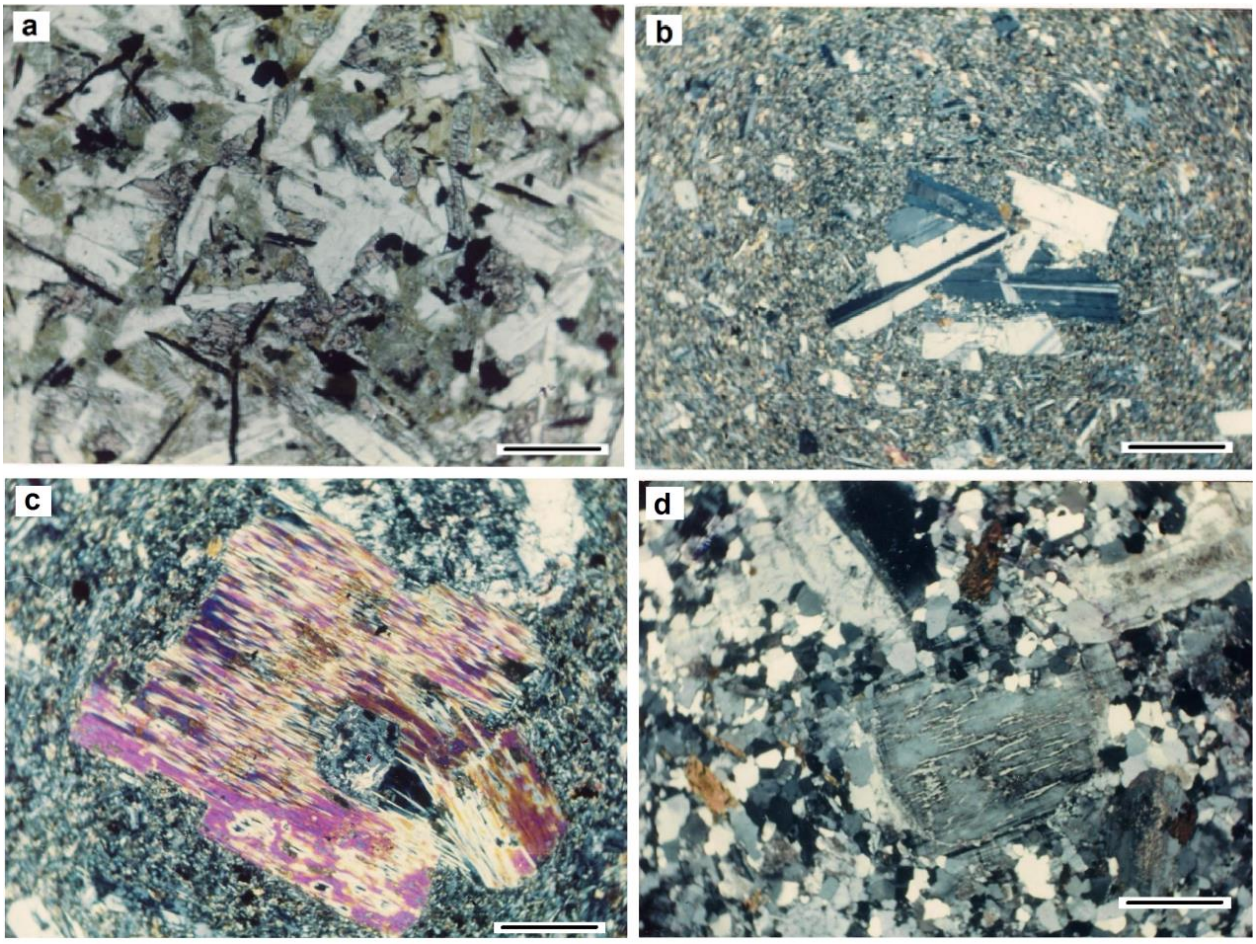

Figure 3) Petrography of the studied dykes. Bar scale is 1 mm for all microphotographs.

The plagioclase phenocrysts form idiomorphic to sub-diomorphic prisms (up to 6.0-0.6 mm long and 4.0-0.4 mm wide), lath-shaped (up to 0.7-0.2mm) and tabular crystals of labradorite composition (An_{50-57}). These crystals are often fresh but some crystals are occasionally altered to sericite. The plagioclase crystals may partially or completely enclose pyroxene (plus

rod-like Fe-Ti oxides) and show a diabasic texture. Intergrangular and amygdaloidal textures are also encountered in the basaltic variety. Deformation effect is manifested by cracking of plagioclase crystals which were later filled with chlorite. Pyroxene is mainly of augite composition in the form of subhedral to anhedral crystals (1.0 X 0.4 mm). They are highly altered to amphibole (actinolite) and/or chlorite. Amphiboles are represented by two varieties; the first is rod-like oxyhornblende (0.6 mm across) which is reddish-brown and highly paleochroic. The second amphibole variety is represented by microphenocrysts of actinolite after pyroxene. The former is fibrous, sometimes flaky, pale green and mostly altered to chlorite. Quartz most probably of secondary origin, occurs as anhedral grains surrounded by secondary fibrous minerals filling amygdales of different shapes. Accessory minerals are mainly represented by idiomorphic to sub-idiomorphic rod-like crystals of ilmenite and titanomagnetite that are sporadically scattered in the groundmass (Fig. 3a), and is closely associated with altered amphiboles. Minute apatite crystals are noticed filling between the other mineral constituents.

3.2- Intermediate dykes

The intermediate dykes are composed of basaltic andesites and trachy-andesite varieties. Megascopically, they are fine-grained massive, brownish, reddish and greenish colors with a characteristics porphyritic texture of plagioclase phenocrysts especially in the trachy-andesite variety. The essential mineral constituents are mainly plagioclase, amphibole, pyroxene, quartz and K-feldspar. Sericite, chlorite, calcite and epidote are recorded as alteration products whereas iron-oxides, apatite and titanite are the main accessories. The plagioclase is commonly present as euhedral to subhedral prismatic crystals (up to 0.9 X 0.3 mm) and short microlaths (up to 0.4 X 0.15 mm). Also, microcrystalline laths are commonly distributed in the groundmass. The plagioclase is of andesine composition (An_{40-47}) and commonly shows zoning and twinning of simple, pericline and lamellar types. Mostly, the plagioclase phenocrysts are highly altered to calcite-epidote admixture and sericite in the core of the crystal. In some instances, the plagioclase phenocrysts tend to clump together forming a glomeroporphyritic texture (Fig 3b). Amphiboles are represented by two varieties: the first is hornblende of euhedral to subhedral prismatic crystals (up to 0.7 X 0.4 mm) of green color, illustrates simple twinning. The second amphibole variety is actinolite of pale green color of fibrous form. The pyroxene phenocrysts are subhedral prismatic crystals (up to 0.9 X 0.6 mm), highly altered to calcite and chlorite. Potash feldspar is rarely encountered and occurs as small anhedral crystals forming a graphic intergrowth with quartz. The groundmass is mainly composed of plagioclase lath-like microlites (up to 0.4 X 0.15 mm) which are highly altered, particularly in the core of the crystals. Euhedral to subhedral microcrystalline prismatic crystals of hornblende (up to 0.3 X 0.1 mm) are highly altered to pale green secondary actinolite (Fig 3c) and/or chlorite. Some small quartz, calcite and epidote veins are noticed cutting the groundmass. Fe-Ti oxides, apatite and titanite are the main accessories around the secondary minerals.

3.3-Felsic dykes

The felsic dykes are mainly of rhyolites and rhyodacites composition which megascopically exhibit pale pink to pinkish-brown and white colors. They are characterized by porphyritic (the most abundant), granophyre and aplitic (sugary) textures. The main constituent minerals are: Quartz, K-feldspar, plagioclase feldspar, biotite and few muscovite. Iron-oxides, apatite and titanite are accessory minerals. Additionally, secondary minerals occur as sericite, chlorite and clayey materials. Quartz is the most abundant constituent, occurs as euhedral to subhedral phenocrysts (average diameter 0.7 mm) embedded in a fine-grained

groundmass mostly of spherulitic quartz and K-feldspar together with iron-oxides as stains. Potash feldspar crystals are mainly subhedral phenocrysts (1.5 x 0.9 mm) of orthoclase composition (An_{12}), form intergrowth with quartz that illustrates granophyric and micrographic textures. Simple lamellar twinning exhibit by fresh homogeneous k-feldspar crystals together with some perthitized which are partially corroded by the groundmass components in the granite porphyry variety (Fig. 3d). Altered K-feldspar crystals show clayey materials. Plagioclase feldspar are represented by euhedral to subhedral prismatic crystals (up to 0.8 x 0.4 mm), sometimes illustrate lamellar twinning but with no zoning. They are highly altered to sericite. Biotite is the main ferromagnesian mineral encountered and represented by flakes (0.3 mm across) of green and pale brown colors, partially or completely altered to chlorite. The groundmass is mainly composed of fine grains of quartz, K-feldspar, plagioclase feldspar, and minute flakes of biotite, muscovite and chlorite together with titanite fragments.

4–Whole-rock geochemistry

4.1- Analytical methods

The present study is based on 27 samples, collected mainly from the dyke swarms in NW Sinai. After the detailed petrographic study, representative15 samples of mafic dykes, 5 samples of intermediate dykes and 7 samples of felsic dykes were selected for major and trace element analyses. Both major and trace elements were analyzed using Sequential Spectrometer PW 2400 XRF at the Polish Geological Institute of Geology, Warsaw. Concentrations of major elements were obtained on fused lithium tetraborate discs whereas the loss on ignition (L.O.I) was determined by heating powdered samples for more than 50 minutes at 1000°C. Samples were prepared for trace-element analysis by making pressed powder pellets. The accuracy and precision of the analytical results were found to be 1-3% for major elements and 5-10% for trace elements.

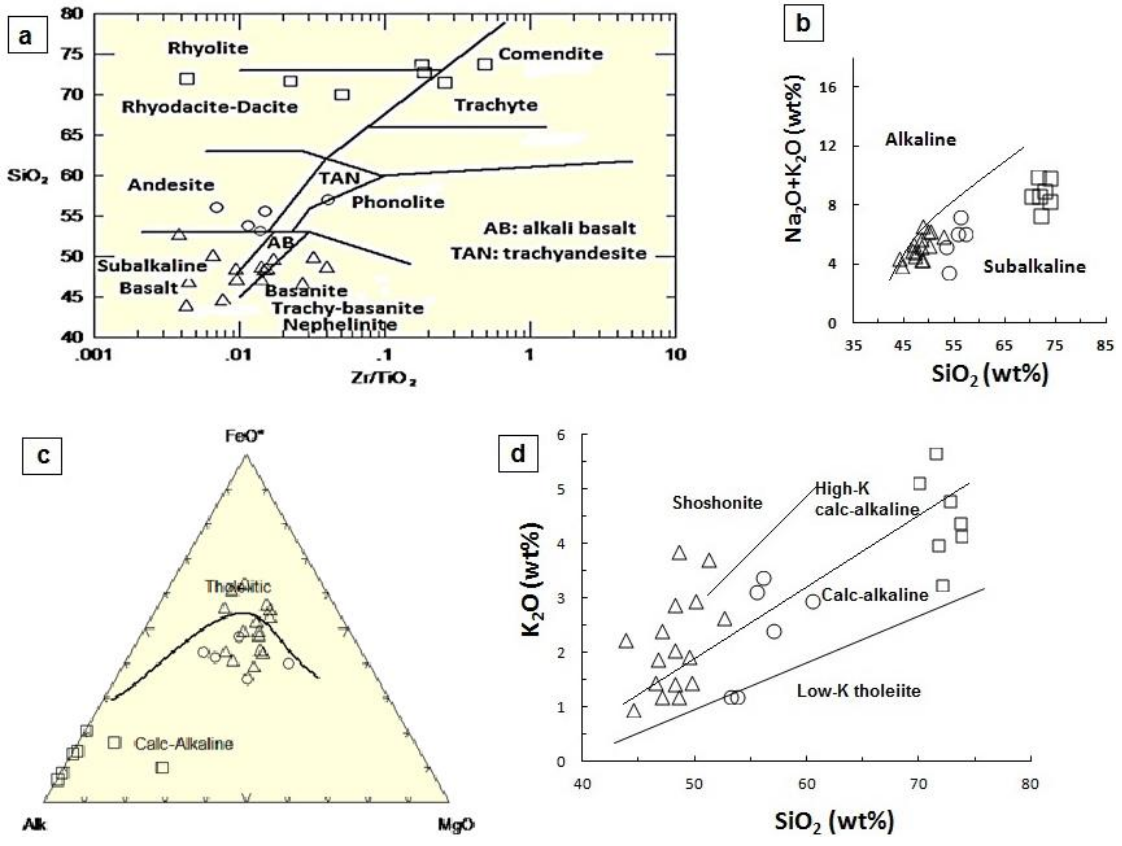

***Fig. 4**: Geochemical classification diagrams for NW Sinai dyke swarms. a) Zr/TiO_2 versus SiO_2 (Winchester and Floyd, 1977). b) SiO_2 vs Na_2O+K_2O (Irvine and Baragar, 1971). c) AFM diagram (Irvine and Baragar, 1971) d) SiO_2 vs K_2O (Peccerillo and Taylor, 1976). Symbols: Δ: mafic dykes; ○: intermediate dykes and □: felsic dykes*

4.2- Classification and magma series of the investigated dykes

Petrographic studies of the investigated dyke swarms indicate that they are slightly altered.Geochemical Classification by using immobile trace elements is very useful in this case. Using Zr/TiO_2 versus SiO_2 diagram (Fig. 4a) after Winchester and Floyd (1977) shows that the investigated mafic dyke swarms mainly occupy sub-alkaline basalt, alkaline basalt and basanite-nephelinite fields while the intermediate and felsic dyke samples plot mainly in the andesite, rhyodacite and rhyolite-trachyte fields, respectively.The investigated dyke swarms are mainly plot in the sub-alkaline field while few mafic samples occur at the boundary line between alkaline and sub-alkaline after Irvine and Baragar (1971)(Fig.4b). The dykes define a transitional trend between calc-alkaline and tholeiitic affinity on the AFM diagram of Irvine and Baragar (1971)(Fig. 4c). On the SiO_2 versus K_2O diagram (Fig. 4d) after Peccerillo and Taylor (1976), the investigated dyke swarms are classified into medium-K and high-K with high-K affinities in the evolved felsic dykes.

4.3- Major and trace element characteristics

The investigated dyke swarms show a wide compositional range from mafic (43.75-49.5 wt % SiO_2), intermediate (52.55–60.49 wt % SiO_2) to felsic (70-73 wt% SiO_2). The mafic dyke swarms are mostly silica undersaturated (nepheline normative) while the intermediate and felsic dykes swarms are silica saturated (quartz and olivine normative)(Table 1). The felsic dyke swarms exhibit corundum normative reflecting their peraluminous nature.

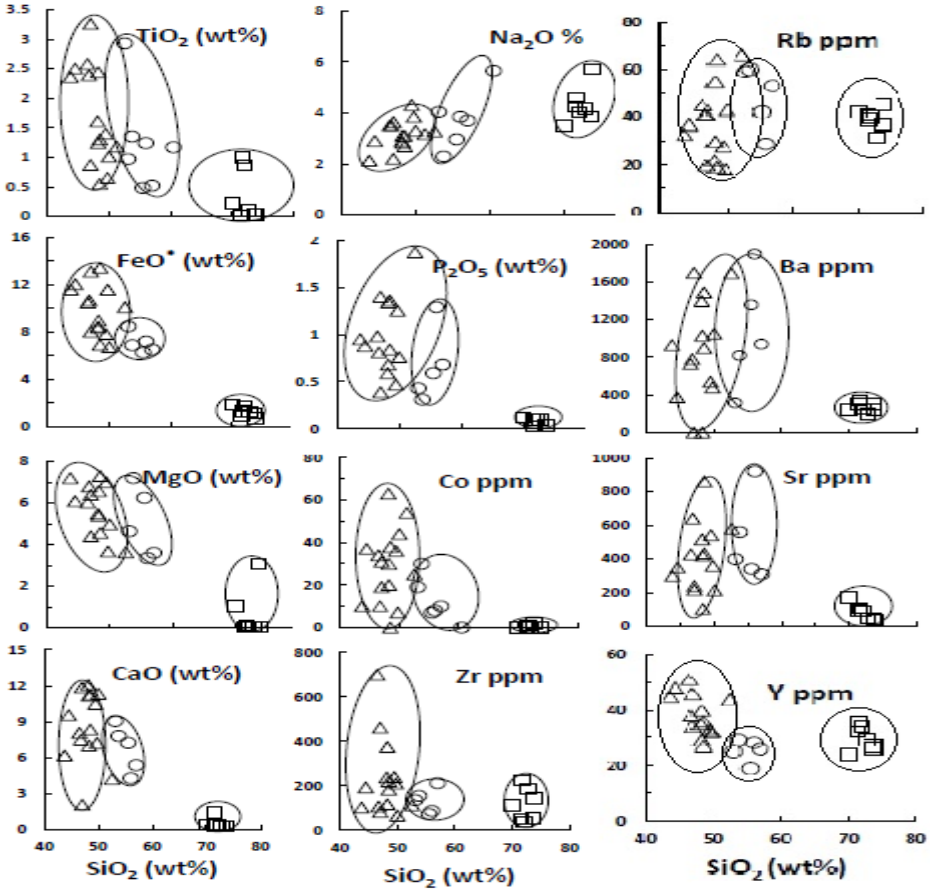

Figure 5) Harker's diagrams showing variation of some major and trace elements vs SiO_2. Symbols as in Fig. 4.

Harker variation diagrams of selective major and trace elements (Fig. 5) illustrate that with increasing SiO_2, the concentrations of TiO_2, FeO^*, MgO, CaO and P_2O_5 tend to decrease while Na_2O and K_2O (not shown) increase. The compatible elements (Co and Y) show a sharp depletion trend with increasing SiO_2 (Fig. 5), whereas the incompatible elements (Rb, Ba, Zr and Sr) show a scattered pattern. The Na_2O contents are generally higher than K_2O in the investigated dyke swarms. Figure 5 elucidates that the mafic; intermediate and felsic dyke samples have a separate groups and not related to each other. This compositional gaps between the three mafic-intermediate and felsic dyke samples; may be interpreted as due to the presence of three independent magmas or may be due to a period of magmatic paucity (Stern *et al*.,1988; El-Gaby *et al*., 1989; Helba, 1989; El-Nisr 1990).

4.4- Incompatible trace elements patterns

A discrimination pattern based on N-MORB (Pearce, 1983) normalized trace element abundances is illustrated in Figure (6 a, b and c).

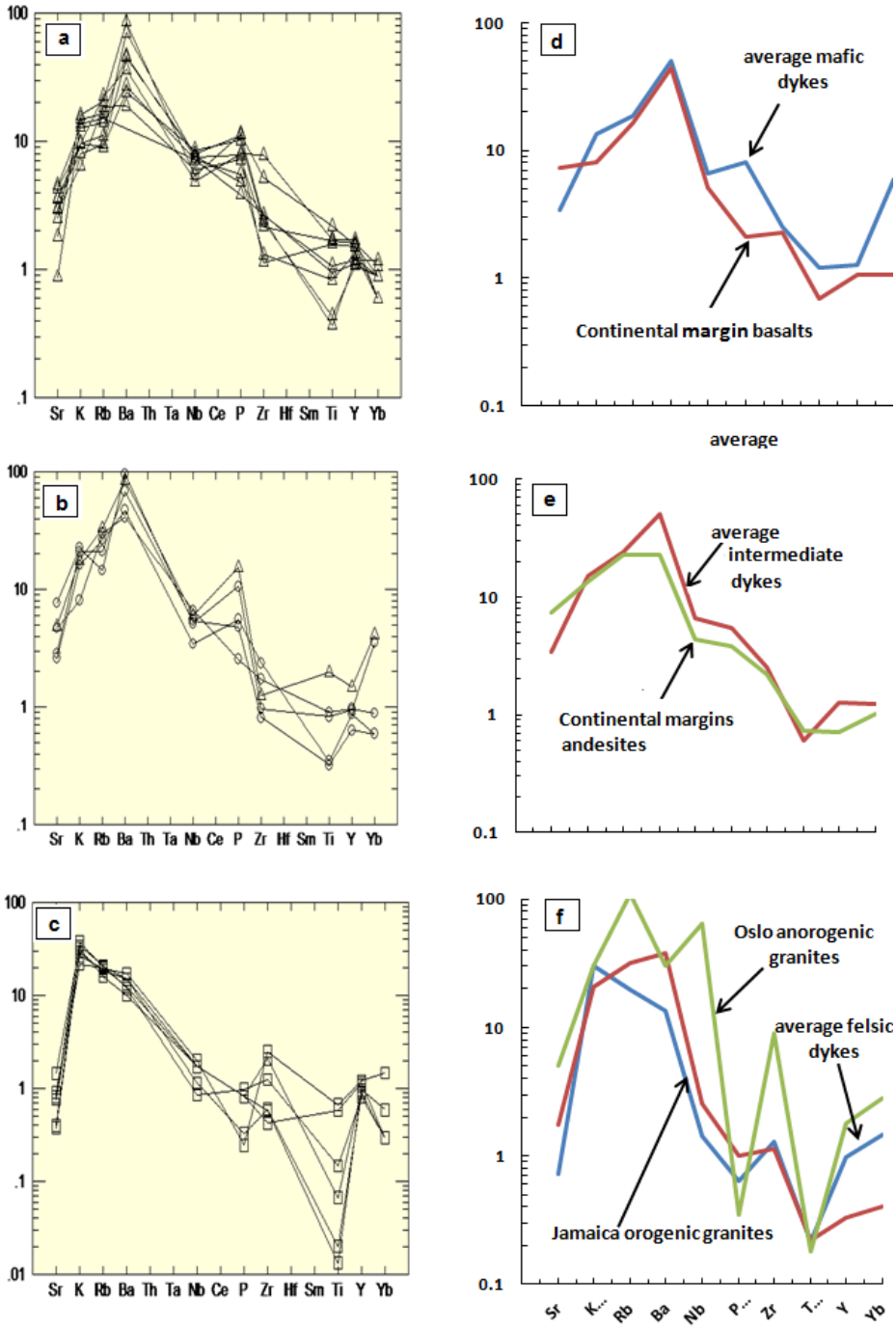

Figure 6) N-MORB normalized trace element abundances (Pearce, 1983). a) Mafic dykes, b) intermediate dykes, c) felsic dykes, d) Comparison with continental margin basalts, e)Comparison with continental margin andesites, f) Jamaica orogenic granites and Oslo anorogenic granites.

The analyzed dykes show an inclined smooth pattern (i.e. enrichment in large-ion lithophile elements (LILE) relative to (HFSE) and are characterized by negative Nb and Ti anomalies (Figs. 6 a, b and c). The felsic dyke samples illustrate similar pattern to the mafic and intermediate dykes but with lower HFSE contents and extreme depletion for P and Ti (Fig. 6c). The average mafic, intermediate and felsic dyke samples are compared with the continental margin basalts after Ewart (1982), the calc-alkaline high-K andesites from active continental margins after Pearce (1983) and Jamaica orogenic granites together with Oslo anorogeneic granites (Pearce *et al.*, 1984); respectively (Figs. 6d, f, and e). A close similarity is shown between the investigated dyke rocks and the previously-mentioned averages (Figures 6d, f, and e) except for the anorogenic granites.

5–Discussion

5.1- Tectonic setting

The investigated mafic dyke swarms fit well with the characteristics of within-plate continental basalts as shown by the Zr/Y versus Zr (Pearce and Norry, 1979)(Fig. 7a).The calc-alkaline rocks developed in an island-arc setting and active continental margins setting (Pearce *et al*., 1984 and Thompson *et al*., 1984). Friz-Töpfer (1991) concluded an active continental margin to an intra-continental setting signature for the dyke swarms of Sinai. The investigated mafic and intermediate dyke samples plot in the continental margin basalt field (Pearce and Norry, 1979) (Fig. 7b). This relation was confirmed by using the SiO_2 versus the Nb diagram (Fig. 7c) after Pearce and Gale (1977). Most of the intermediate and mafic dyke samples straddle the overlap area between the within-plate magma and the arc-magma, while the felsic samples plot in the field of arc-magma. By using the relation between (Y+Nb) versus Rb after Pearce *et al*., (1984); the investigated felsic dyke samples plot in the volcanic-arc field (Fig. 7c) and within-the post collision granite field after Pearce (1996).

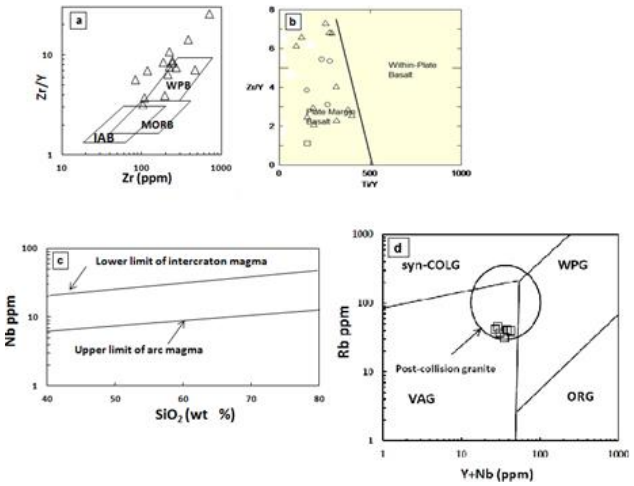

Figure 7) Tectonic discrimination diagrams for NW Sinai dyke rocks. a) Zr vs Zr/Y (Pearce and Norry, 1979). WPB: within-plate basalt; MORB: mid-oceanic ridge basalt and IAB: island-arc basalt. b) Ti/Y vs Zr/Y (pearce and Norry, 1979). c) SiO_2 versus Nb (Pearce and Gale, 1977). d) (Y+Nb) vs Rb (Pearce et al., 1984). Syn-COLG: syn-collision granite; VAG: volcanic-arc granite; ORG: oceanic ridge granite and WPG: within-plate granite. Symbols as in Fig. 4.

5.2- Magma sources of the investigated dykes

Mafic rocks that are arguably part of the extensional-related tectono-magmatic event which had affected eastern Egypt during the final stages of the Neoproterozoic crustal evolution are the dyke swarms (Stern *et al*., 1984; Stern and Voegeil, 1987). These dykes are similar to the Dokhan volcanic in being dominated by high-K andesites and have the same geochronological data 633-550 Ma for Dokhan volcanic in Sinai (Bielski *et al*., 1979; Segev, 1987; Moghazi, 1994 and Wilde and Youssef, 2000, 2002) and 591± 9 Ma for the investigated dykes (Stern and Manton, 1987).The Late Neoproterozoic post collisional stage of tectonomagmatic evolution of the ANS commenced at ~ 620 Ma, the transition from convergence to extension occurred ~ 600 Ma (Stern, 1994; Garfunkel, 1999; Genna *et al*., 2002b and Jarrar *et al*., 2003) and was finally followed by a stable craton and platform setting (Garfunkel, 1999). Available U-Pb zircon data

Table 1) Chemical data (major and trace elements) of bimodal dyke swarms of NW Sinai-Egypt mafic dykes.

	Mafic Dykes															Av. Mafic
	Basaltic												Trachybasalt			Dykes
	187	221	225	b	176a	87	157	160	27	228	213	103	96	3	88	
Major oxides (Wt. %)																
SiO_2	43.8	44.5	46.5	46.8	47	47	48.2	48.3	48.3	48.5	52.6	49.5	49.8	48.5	50	47.93
Al_2O_3	16.1	15	16.6	15.3	15.5	16.8	14.2	15.6	15.8	12.5	14	15.6	13	14.2	15.3	15.02
TiO_2	2.36	2.5	2.58	2.39	3.26	0.87	1.61	1.24	2.44	0.55	2.93	1.4	0.65	1.3	1.01	1.81
Fe_2O_3	7.17	4.08	5.57	4.46	9.45	1.36	2.66	2.8	7.84	3.85	8.91	2.39	10.9	7.2	4.46	5.54
FeO	6.54	9.16	6.56	7.52	6.47	7.04	6.48	6.48	3.46	10.7	3.84	6.12	3.96	1.86	3.58	5.99
MgO	7.2	6.09	6.03	6.8	4.4	6.4	5.48	6.58	5.38	7.3	3.63	7	3.67	4.56	4.97	5.70
CaO	6.18	9.54	8.06	7.5	2.07	11.9	12.1	11.2	7	8.35	4.24	10.5	7.23	11.3	11.3	8.55
Na2O	2.13	2.9	3.5	3.5	2.2	3.64	2.89	3.1	2.83	3.1	3.27	4.31	3.85	2.69	3.3	3.15
K2O	2.23	0.96	1.45	1.88	2.4	1.2	1.44	2.05	2.89	1.2	2.65	1.93	1.45	3.85	2.95	2.04
P_2O_5	0.95	0.88	0.98	0.81	1.4	0.39	0.59	0.68	1.34	1.36	1.87	0.47	1.25	0.84	0.76	0.97
MnO	0.34	0.24	0.19	0.2	0.25	0.17	0.25	0.2	0.22	0.24	0.15	0.21	0.15	0.24	0.12	0.21
L.O.I.	5.91	2.73	2.45	2.92	4.52	3.31	4.39	2.49	3.09	2	2.79	1.27	4.88	3.85	3.49	3.34
Total	101	98.5	100	100	99	100	100	101	101	99.7	101	101	101	100	101	100.24
C.I.P.W																
Q	0	0	0	0	17.2	0	0	0	4.56	0	7.26	0	7.34	0	0	2.42
Or	14.3	5.92	8.77	11.2	16	7.36	8.87	12.3	17.3	7.22	16.2	11.3	9.16	23.8	17.4	12.47
Ab	13.5	20.8	32.2	33	22.3	14.9	23.9	18.8	25.8	14.3	35	22.6	37.1	15.2	16.9	23.07
An	29.9	26.6	29.8	23.4	1.26	26.7	22.4	22.9	24.9	17	13.9	17.4	14.8	16.1	18.2	20.34
Ne	3.21	2.63	0	0	0	9.14	0.87	4.28	0	1.34	0	9.38	0	6	7.62	2.96
C	0	0	0	0	11	0	0	0	0	0	0	0	0	0	0	0.73
Di	34.1	26.3	3.64	0	0	29	25.3	27.1	0	35.2	0	24.8	0	0	30.4	15.73
Wo	0	0	0	0	0	0	0	0	0.57	0	3.2	0	5.95	17.1	0	1.79
Hy	0	0	2.87	10.2	17.2	0	0	0	15.1	0	10.4	0	1086	13.2	0	77
Ol	0.7	5.06	13	13.2	0	9.21	12.8	8.37	0	4.61	0	11	0	0	2	5
Mt	11.2	6.18	5.96	4.89	11.1	2.04	4.03	4.13	7.09	5.71	0.36	2.46	8.78	4.45	4.65	6
He	0	0	0	0	0	0	0	0	0.82	0	0.84	0	2.26	2.27	0	0
Il	1.88	4.96	1.67	1.16	0.79	0.66	0.23	0.48	1.06	1.06	0.81	0.15	0.97	0.14	1.4	1
Ap	0.25	2.13	2.1	1.76	3.31	0.94	1.41	1.6	2.85	3.52	4.05	0.96	2.81	1.83	1.57	2
Trace elements (ppm)																
Cr	151	217	253	240	4	251	460	315	110	90	945	305	82	163	287	258
Ni	83	73	98	68	48	110	345	430	38	64	58	43	46	8	128	109
Co	10	37	34	10	19	31	63	20	30	n.d	25	36	7	38	n.d	28
V	275	228	134	306	345	408	213	410	178	336	194	246	330	260	424	286
Sc	32	41	27	26	87	45	38	27	32	44	31	31	40	15	23	36
Rb	33	37	45	41	41	20	22	30	55	19	66	28	18	64	43	37
Cu	63	38	44	24	22	23	73	64	33	25	35	5	5	72	22	37
Y	45	48	51	38	46	34	35	40	29	36	44	33	32	27	32	38
Yb	2	3.6	2	2.5	3	2	4	2	2	3	14	3	3	3	1	3
Nb	26	21	17	20	19	24	27	25	19	28	21	25	30	21	22	23
Zr	102	193	700	107	462	83	238	117	375	220	112	240	210	183	66	227
Sr	300	350	428	640	217	240	517	104	420	433	580	542	360	860	214	414
Ba	930	375	730	780	1700	n.d	1400	n.d	1030	898	1695	540	480	1490	1050	1008
Zr/TiO_2	0	0.01	0.03	0	0.01	0.01	0.01	0.01	0.02	0.04	0	0.02	0.03	0.01	0.01	0
Ti/Y	453	312	574	509	327	361	358	455	562	115	710	295	120	364	296	387
Zr/Y	3.26	4.02	26	3.8	7.21	5.76	8.84	7.17	14.4	7.71	4.53	8.45	6.48	8.55	3.25	8
Na_2O+K_2O	4.36	3.86	4.95	5.31	4.6	4.84	4.34	5.14	5.72	4.3	6.4	6.24	5.3	6.54	6.25	5
Mg≠	38.4	33.6	36.6	39	25.2	44.5	39.7	43.8	37.6	35.2	26.5	47.3	24.1	39.8	42.6	37

n.d : not detected

Mg ≠ = 100 MgO/(MgO + FeO^{tot})

Table 1) Continued

	Intermediate Dykes					Av. Inter.	Felsic Dykes							Av.Felsic
	Basaltic-andesite			Trachyandesite		Dykes								Dykes
	T5	99	84c	167	165		84b	222	127	84a	145	200	T10	
Major oxides (Wt. %)														
SiO_2	53.1	53.75	57	55.5	56	55.07	70	71.5	71.65	72	72.75	73.65	73.75	72.19
Al_2O_3	17.5	17.33	15.1	13.25	16.03	15.842	16.39	13.57	15.38	15.73	13.24	14.23	14.6	14.73
TiO_2	0.97	1.35	0.52	0.48	1.24	0.912	0.22	0.02	1	0.87	0.1	0.03	0.03	0.32
Fe_2O_3	2.35	0.99	2.13	2.52	4.12	2.422	0.92	0.09	1.22	1.03	1.21	0.7	0.14	0.76
FeO	6.8	6.16	5	4.48	4.28	5.344	1.16	0.84	0.4	0.96	0.36	0.6	0.56	0.70
MgO	4.64	7.2	3.6	6.25	3.35	5.008	1.03	0.03	0.1	0.03	0.03	3.06	0.03	0.62
CaO	9.05	7.8	5.37	7.24	4.28	6.748	0.4	1.4	0.34	0.4	0.28	0.28	0.28	0.48
Na2O	4.04	2.29	3.7	2.96	3.85	3.368	3.5	4.24	4.59	4.04	4.17	3.85	5.72	4.30
K2O	1.2	1.2	2.41	3.13	3.37	2.262	5.12	5.66	3.99	3.25	4.79	4.39	4.15	4.48
P_2O_5	0.43	0.31	0.68	0.59	1.29	0.66	0.12	0.1	0.03	0.1	0.1	0.04	0.04	0.08
MnO	0.15	0.25	0.2	0.18	0.19	0.194	0.02	0.01	0.01	0.03	0.01	0.01	0.01	0.01
L.O.I.	1.78	1.3	3.4	3.83	2.9	2.642	1.57	1.64	1.01	2.48	0.72	1.25	0.01	1.24
Total	102.01	99.93	99.11	100.4	100.9	100.472	100.5	99.1	99.72	100.9	97.76	102.1	99.32	99.91
C.I.P.W														
Q	0	4.04	8.86	7.26	8.5	5.73	27.53	20	29.8	35.19	30.52	29	24.06	28.01
Or	7.07	7.16	14.92	16.21	20.5	13.17	30.38	33.47	23.79	19.23	29.4	26	24.6	26.70
Ab	34	20.7	34.83	34.99	35.53	32.01	29.6	32	38.79	34.15	36.29	32	48.4	35.89
An	26.5	36.99	18.29	13.9	13.21	21.78	1.22	1.23	0	1.34	1.37	0.99	1.13	1.04
Ne	0	0	0	0	0	0	0	0	0	0	0	0	0	0
C	0	0	0	0	0	0	4.63	0	3.59	5.87	0.67	2.5	0.26	2.50
Di	13	0	3.96	0	0	3.39	0	0	0	0	0	0	0	0
Wo	0	0	0	3.2	0	0.64	0	7.5	0	0	0	0	0	1.07
Hy	11.12	29.18	14.54	10.36	12	15.44	3.6	1.53	0.39	0.93	0.07	8.12	0.93	2.22
Ol	2.15	0	0	0	0	0.43	0	0	0	0	0	0	0	0.00
Mt	3.48	1.04	2.34	0.36	4.42	2	1.34	0.14	0	1.64	0.88	1.02	0.2	0.75
He	0	0	0	0.84	0	0	0	0	1.38	0	0.6	0	0	0.28
Il	1.86	1.52	0.75	0.81	1.78	1	0.43	0.04	0.9	1.6	0.2	0	0.07	0.46
Ap	1	1.64	1.49	4.05	2.76	2	0.27	0.23	0.06	0.13	0.01	0.1	0.09	0.13
Trace elements (ppm)														
Cr	280	418	146	149	193	237	198	177	301	162	330	230	226	232
Ni	66	51	72	50	64	61	78	70	170	82	139	125	94	108
Co	19	30	10	7	8	15	n.d	n.d	1	n.d	2	n.d	n.d	2
V	206	194	362	256	45	213	51	n.d	n.d	15	n.d	n.d	n.d	33
Sc	25	21	21	14	17	20	4	2	3	3	3	3	2	3
Rb	59	60	53	42	29	49	42	41	39	40	32	37	45	39
Cu	245	40	14	72	4	75	2	n.d	10	2	n.d	n.d	1	4
Y	25	29	26	19	28	25	24	32	36	34	29	27	26	30
Yb	2	3	2	2	12	4	1	n.d	5	1	2	1	1	2
Nb	19	23	12	19	18	18	3	6	7	6	6	4	3	5
Zr	136	155	212	73	87	133	112	52	224	38	187	54	146	116
Sr	400	560	310	342	920	506	174	97	108	91	48	45	42	86
Ba	315	820	940	1360	1900	1067	240	300	345	250	200	300	240	268
Zr/TiO_2	0.014	0.011	0.04	0.015	0.007	0	0.082	4.53	0.022	0.08	0.31	0.613	0.699	1
Ti/Y	228	347	148	156	237	223	162	9.52	2950	1040	25	100	50	620
Zr/Y	5.33	6.65	10	3.92	3.95	6	14	n.d	112	7.6	93.5	54	73	59
$Na_2O+K_2($	5.24	3.49	6.11	6.09	7.22	6	8.62	9.9	8.59	7.29	8.97	8.25	9.88	9
Mg≠	35.47	51.24	35.68	50.03	31.87	40.86	36.36	3.22	7.39	1.75	2.43	73.75	4.36	18.46

n.d : not detected

Mg ≠ = 100 MgO/(MgO + FeO^{tot})

(Beeri-Shlevi *et al*., 2009) show that in the SW Sinai the emplacement of calc-alkaline suites lasted from ~ 620 to 597 Ma. The spider diagram of trace elements (Fig. 6) shows a Nb-

negative anomaly; indicate arc signature (Hollings and Wyman, 1999; Gill, 2010).These feature of the study dyke swarms may be inherited from the partial melting of enriched lithospheric mantle which formed from a previous subduction episode in the ANS. Therefore, the study dyke swarms represent transitional tectonic setting between subduction and extension phases (Figs. 6 and 7).

The pronounced feature in figure (5), is the presence of two compositional gaps between the mafic and the intermediate dykes in one hand and between the intermediate and the felsic dykes on the other hand. This means that each dyke variety has its own magma; which evolved separately.The most mafic rock ($SiO_{2=}$ 47wt%) - in the investigated dykes-is not primary; Mg# and Ni content are low (Mg# = 44.5, Ni = 110 ppm) to be in equilibrium with a mantle composition (Green, 1980) but include melt which perhaps has been affected by some degree of fractional crystallization and/or crustal contamination. Crustal contribution to calc-alkaline magmas in the northern ANS was elucidated by many workers (Azer, 2007; Abu Anbar, 2009; Beeri-Shlevi *et al*., 2009a, b and Eyal *et al*., 2010). Therefore, the studied dykes are derived from mafic mantle magmas with slight crustal contamination.

Inspection of Table 1 reveals that Ni and Cr contents (109, 258 ppm on average; respectively) are extremely depleted in the analyzed mafic dykes. Such a drastic depletion of Ni and Cr could be explained by small degree of partial melting of heterogeneous mantle source followed by fractional crystallization (Fitton and Upton, 1985).According to Farahat and Azer (2011) and Azer (2013), the post-collisional magmatism in Sinai caused by fractional crystallization of a parental magma derived through partial melting of a juvenile crust that resulted in the formation of ring-like complexes at Gabal Serbal (~605-580 Ma) and Saint Katherina (~610-580 Ma). Also, a strong enrichment of LILE (Ba and Sr) coupled with enrichment of the incompatible elements Zr and Ti relative to Y and Yb; leave little doubt that these mafic dykes are the products of a limited degree of partial melting. The Sr initial isotope ratio of one basic dyke from west El-Sheikh is 0.7034 ± 2(age 591 ± 9, Stern and Manton, 1987) and this fit quite well those of the country rocks (paragneiss and granites), i.e. 0.7032 – 0.7039 (Stern and Manton, 1987). These isotope data indicate time integrated depleted source material. Partial melting of the investigated mafic dyke samples from a mantle source was tested by using the relation between Ba/Ca versus Sr/Ca after Lopez-Esobar *et al*., 1985 (Fig. 8b). This diagram illustrates a small degree partial melting (~ 1.8) is obtained from a mantle source to produce the mafic dykes (Fig. 8).

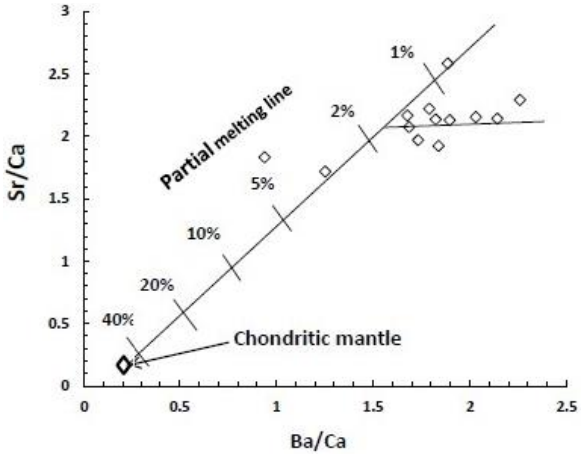

Figure 8) Ba/Ca vs Sr/Ca in the NW Sinai mafic dykes. The partial melting line is defined by primitive basalts from island arc regions (Lopez-Escobar et al., 1985). The intersection of the two lines defines the possible composition of primitive magma of the investigated mafic dykes.

Fractional crystallization might be accompanied by considerable partial melting or minor crustal contamination during the development of magmas in the northwestern ANS (Jarrar *et al*., 2004; Azer *et al*., 2012). The selective enrichment of large ion-lithophile elements (Rb, Ba, K) relative to high field strength elements (Zr, Nb, Y, Ti) along with Nb trough (Fig. 6), are generally considered to be critical features of volcanic arc magmas (Pearce, 1983) as well as of calc-alkaline rocks from destructive plate

boundaries like, continental margin (Thompson *et al*., 1984). The investigated intermediate dykes most probably produced by fractional crystallization process(es) from a previously partially melted basaltic magma. Fractional crystallization processes governs the evolution of the investigated intermediate magma. The geochemical variation trends (Fig. 5, Table 1) for the intermediate dyke samples show a decrease of TiO_2, FeO^*, CaO and MgO together with Co consistent with the removal of pyroxene, amphibole from the melt in the magma chamber before their eruption. Also, the depletion of CaO and P_2O_5 coupled with Sr, Y and Zr (Fig. 5) suggest fractional crystallization of plagioclase, apatite and zircon.

A wide spread late-to post orogenic calc-alkaline (630–590 Ma) and alkaline (610-580 Ma) magmatism intruded the northern part of the ANS, with both magma types emplaced between 610-590 Ma (Beyth *et al*., 1994; Merrt, 2003; Beeri-Shlevi *et al*., 2009a; Avigad and Gvirtzman, 2009; Eyal *et al*., 2010; Azer *et al*., 2010). Many post-orogenic batholiths in Sinai (610-590 Ma) may be formed during crustal thinning and extension (Beeri-Shlevi *et al*., 2009, 2010 and Eyal *et al*., 2010).

Since the investigated felsic dyke swarms has its own separate magma; it most probably formed by partial melting of mafic lower crust then the fractional crystallization process was dominated to produce the most evolved samples.

Although, the geochemical signatures for the investigated dykes exhibit negative Nb-anomalies (Fig. 7) which characterize magmas of subduction processes. The investigated dyke swarms may not related to subductionprocesss for the following criterias: a) the long period of subduction (> 300 Ma) in eastern Egypt, prior to the onset of the dyke magmatism, b) the predominance of dyke swarms of the same age as the Dokhan volcanic (Stern and Voegeli, 1987) as well as the synchronous timing of the Dokhan volcanic with some ring complexes in the northern part of the Eastern Desert (i.e. the Wadi Dib ring complex in northern Egypt dated at 578 Ma (Frisch and Abdel Rahman, 1999), and c) the reported ages for the A-type granites which were cut by the dyke swarms vary between 610 and 550 Ma, which are very similar to those of Dokhan Volcanic 620-550Ma.Therefore, the tectonic setting of the investigated dyke swarms together with their crosscut relationships, most probably formed in a transitional tectonic setting from arc magma to within-plate magma.The investigated dyke swarms of Sinai are emplaced under tensional environment during a transitional period between volcanic-arc and within-plate regimes in the Late Neoproterozoic.

6–Conclusions

The following are the main concluding remarks of this study:

a) Petrographically, the investigated dyke swarms of NW Sinai, Egypt are subdivided into mafic (dolerite, basalt, trachy-basalt), intermediate (basaltic-andesite, trachy-andesite) and felsic (rhyodacite, rhyolite) varieties.

b) Geochemically, the dyke swarms show a wide compositional range from mafic (43.75 – 49.5 wt% SiO_2), intermediate (52.55 – 60.49 wt% SiO_2) to felsic (70–73 wt% SiO_2). The investigated dyke samples are calc-alkaline with weak alkaline affinity to some mafic samples.

c) A compositional gaps exist between the mafic-intermediate dyke samples on one hand and the intermediate and felsic samples on the other hand; this is attributed to the presence of more than one magma pulse or due to a period of magmatic paucity.

d) Although the geochemical characteristics for the dyke swarms indicate a subduction-related environment their tectonic setting together with field crosscut relationships, confirm that these dykes are most probably formed in a transitional tectonic setting from arc magma to within-plate magma.

e) The chemical features for extensional-related volcanics; indicate an enriched lithospheric mantle source where the long period of subduction (~ 300 Ma) in eastern Egypt prior to the onset of the dyke magmatism resulted in LILE enrichment of the sub-continental mantle lithosphere.

f) The investigated mafic dykes were produced by a small degree partial melting (~ 1.8) of enriched lithospheric mantle which formed from a previous subduction episode then followed by fractional crystallization processes.

g) The investigated intermediate dykes most probably produced by fractional crystallization process(es) from a previously partially melted basaltic magma. Fractional crystallization processes governs the evolution of the investigated intermediate magma due to the removal of pyroxene, amphibole, plagioclase, apatite and zircon from the melt in the magma chamber before their eruption.

h) The felsic dykes most probably evolved by partial melting of lower mafic crust which led to the formation of rhyolitic magma. the studied dykes are derived from mafic mantle magmas with slight crustal contamination.

Acknowledgments:

The authors would like to thank Dr. Kamal A. Ali, Dr. H. Mirnejad and Prof. A. M. H. Asran for their appreciate comments which help us to improve manuscript.

References:

Abdel-Rahman, A. M. 1996. Pan-African volcanism: petrology and geochemistry of the Dokhan Volcanic suite in the northern Nubian Shield. Geological Magazine: 133, 17–31.

Abou El-Maaty, M.A., Ali-Bik, M.W., Sadek, M.F. 2011. Petrogenesis and age dating of continental Mesozoic basalts, Um Bogma area, Sinai, Egypt. Neues Jahrbuch für Mineralogie Abhandlungen: 188, 199–210.

Abu Anbar, M. M. 2009. Petrogenesis of the Nesryin gabbric intrusion in SW Sinai, Egypt: new contributions from mineralogy, geochemistry, Nd and Sr isotopoes. Mineralogy and Petrology: 95, 87–103.

Avigard, D., Gvirtzman, Z. 2009. Late Neoproterozoic rise and fall of the northern Arabian-Nubian Shield: the role of the lithospheric mantle deamination and subsequent thermal subsidence. Tectonophysics: 477, 217–228.

Azer, M.K. 2007. Tectonic significance of late Precambrian calc-alkaline and alkaline magmatism in Saint Katherina area, southern Sinai, Egypt. Geologica Acta: 5, 255–272.

Azer, M. K., Stern, R. J., Kimura, J.I. 2010. Origin of a Late Neoproterozoic (605± 13 Ma) intrusive carbonate-albitite complex in Southern Sinai, Egypt. International Journal of Earth Science: 99, 245–267.

Azer, M.K. 2013. Late Edicaran (605-580 Ma) post-collisional alkaline magmatism in the Arabian-Nubian Shield: a case study of Serbal ring-shaped intrusion, southern Sinai, Egypt. Journal of Asian Earth Sciences: 77, 203–223.

Azer, M.K., Abu El-Ela, F.F., Ren, M. 2012. The petrogenesis of late Neoproterozoic mafic-dyke-like intrusion in south Sinai, Egypt. Journal of African Earth Sciences: 54–55, 91–109.

Beeri-Shlevi, Y., Katzir, Y., Valley, J. W. 2009. Crustal evolution and recycling in a juvenile contenint: isotope ratio of zircon in the northern Arabian-Nubian Shield. Lithos: 107, 169–184.

Beeri-Shlevi, Y., Katzir, Y., Blichert-Toft, Kleinhanns, I. C., Whiteehouse, M. 2010. Nd-Sr-Hf-O isotpe provinciality in the northernmost Arabian-Nubian Shield: implications for crustal evolution. Contributions to Mineralogy and Petrology: 160, 181–201.

Bentor, Y. K., 1985. The crustal evolution of the Arabo-Nubian Massif with special reference to Sinai Peninsula. Precambrian Research: 28, 1–74.

Bielski, M. Jäger, E., Steinitz, G.. 1979. The geochronology of Iqna granite (Wadi Kid pluton), southern Sinai. Contributions to Mineral and Petrology: 70, 159–165.

Beyth, M., Peltz, S., 1992. Petrology and major-element geochemistry of dikes at HarTimna, Southern Israel. Geological Survey of Israel, Report No. GSI/13/92, 39p.

El-Baily, M.Z., Hassen, I. 2012. The late Edicaran (580-590 Ma) onset of anorogenic alkaline magmatism in the Arabian-Nubian Shield: Katherina A-type rhyolites of Gabal Ma'ain, Sinai, Egypt. Precambrian Research: 216, 1–22.

El-Gaby, S., Khudeir, A.A., El-Taky, M. 1989. The DokhanVolcanics of Wadi Queh area, Central Eastern Desert, Egypt. Annals of the Geological Survey of Egypt: 2, 1–18.

Iacumin, M., Marzoli, A., El-Metwally, A., Piccirilo, E. M., 1998. Neoproterozoic dyke swarms from southern Sinai (Egypt): Geochemistry and petrogenesis aspects. Journal of African Earth Sciences: 26, 49–64.

El-Nisr, S.A., 1990. Petrological and geochemical studies of basement rocks in Central Western Sinai, Egypt. Unpublished Ph. D. Thesis, Alexandria University, Egypt, 268 p.

El-Nisr, S.A., Moghazi, A.M., 2001. Geochemistry, petrogenesis and paleotectonic significance of dyke swarms intruding Neoproterozoic basement rocks, south Marsa Alam area, Eastern Desert, Egypt. Bulletin of the Faculty of Science, Assiut University, Egypt: 30, 117–134.

El-Sayed, M. M. 2006. Geochemistry and petrogenesis of the post-orogenic bimodal dyke swarms in NW Sinai, Egypt: constraints on the magmatic-tectonic processes during the late Precambrian. Chemie der Erde: 66, 129–141.

El-Shishtawy, Y.A., 1994. Petrological and geochemical study of granitic rocks around Wadi El-Sheikh, South Western Sinai, Egypt. Unpublished Ph. D. Thesis, Mansoura University, Egypt, 151p.

Ewart, A. 1982. The mineralogy and petrology of Tertiary-Recen torogenic rocks with special reference to the andesite-basaltic compositional range, in: Thorpe, R.S. (Ed.), Andesites, Orogenic Andesites and Related Rocks. John Wiley, Chichester, pp. 25–98.

Eyal, M., Livinovsky, B., Jan, B. M., Zanvilevich, A., Katzir, Y. 2010. Origin and evolution of post-collisional Magmatism : coeval Neoproterozoic calc-alkaline and alkaline suites of the Sinai Penensula. Chemical Geology: 269, 153–179.

Farahat, E.S., Azer, M.K. 2011. Post-collisional magmatism in the northern Arabian-Nubian Shield: the geotectonic evolution of the alkaline suite at Gebel Tarbush, south Sinai, Egypt. Chemie der Erde: 71, 247–266.

Fitton, J.G., Upton, G.G.J. 1985. Alkaline igneous rocks: a review symposium. Journal of the Geological Society of London: 142, 697–708.

Fowler, A.R., Hassen, I., Osman, A.F. 2010. Neoproterozoic structural evolution of SE Sinai, Egypt: II. Convergent tectonic history of the continental arc Kid Group. Journal of African Earth Sciences: 58, 526–546.

Frisch, H., Abdel Rahman, A.M. 1999. Petrogensis of the Wadi Dib alkaline ring complex, Eastern Desert, Egypt. Mineralogy and Petrology: 65, 249–275.

Friz-Töpfer, A. 1991. Geochemical characterization of Pan African dyke swarms in southern Sinai: from continental margin to intra-plate magmatism. Precambrian Research: 49, 281–300.

Jarrar, G. 2001. The youngest Neoproterozoic mafic dyke suite in the Arabian-Nubian Shield: mildly alkaline dolerites from south Jordan- their geochemistry and petrogenesis. Geological Magazine: 138, 309–323.

Jarrar, G. W., Wachendorf, H., Saffarini, G. 1992. A late Proterozoic bimodal volcanic/sub volcanic suite from Wadi Araba. Southwest Jordan. Precambrian Research: 56, 51–72.

Jarrar, G. W., Stern R. J., Saffarini, G., Al-Zubi, H. 2003. Late- and post-orogenic Neoproterozoic intrusions of Jordan: implications for crustal growth in the northernmost segment of the East–African orogeny. Precambrian Research: 123, 295–319.

Jarrar, G., Saffarini, G., G., Baumann, A., Wachendorf, H. 2004. Origin, age and petrogenesis of Neoproterozoic composite dikes from the Arabian-Nubian Shield, SW Jordan. Geological Journal: 39, 157–178.

Garfunkel, Z. 1999. History and paleogeography during the Pan-African orogeny to stable platform transition: reappraisal of the evidence from the Elat area and the northern Arabian –Nubian Shield. Israel Journal of Earth Sciences: 48, 135–157.

Genna, A., Nehlig, P., Le Goff, E., Gguerrot, C., Shanti, M. 2002. Proterozoic tectonism of the

Arabian Shield. Precambrian Research: 117, 21–40.

Gill, R. 2010. Igneous rocks and processes: A practical Guide. Wiley-Blackwell, P. 460.

Green, D.H. 1980. Island-arc and continental building magmatism a review of key geochemical parameters and genetic processes. Tectonophysics: 63, 367–385.

Greiling, R.O., Abdeen, M.M., Dardir, A.A., El-Akhal, H., El-Ramly, M.F., Kamal El-Din, G.M., Osman, A.F., Rashwan, A.A., Rice, A.H.N., Sadek, M. F. 1994. A structural synthesis of the Proterozoic Arabian Nubian Shield in Egypt. Geologische Rundschau: 83, 484–501.

Helba, H.A. 1989. Petrological and geochemical studies of dykes cutting basement rocks in Southwestern Sinai, Egypt. Unpublished M. Sc. Thesis, Alexandria University, Egypt,180p.

Hollings, P., Wyman, D. 1999. Trace elements and Sm-Nd systematics of volcanic and intrusive rocks from the 3 Ga Lumby Lake Greenstone belt. Superior Province: evidence for Archean plume-arc interaction. Lithos: 46, 189–213.

Irvine, T.N., Baragar, W.R.A., 1971. A guide to the chemical classification of the common volcanic rocks. Canadian Journal of Earth Sciences: 8, 523–548.

Kromkhun, K., Foden, J., Hore, J., Baines, G. 2013. Geochronology and Hf isotopes of the bimodal mafic-felsic high heat producing igneous suite from Mt Painter Province, South Australia. Gondwana Research: 24, 1067–1079.

Kröner, A. 1985. Ophiolites and the evolution of the tectonic boundaries in the late Proterozoic Arabian-Nubian Shield of northeast Africa and Arabia. Precambrian Research: 27, 277–300.

Lopez-Escobar, L., Moreno, H., Tagiri, M., Notsu, K., Onuma, N. 1985. Geochemistry and petrology of lavas from San Jose volcano, Southern Andes (33°45`S). Geochemical Journal: 19, 209–222.

Merrt, J. G. 2003. A synopsis of events related to the assembly of eastern Gondwana. Tectonophysics: 362, 1–40.

Mohamed, F.H., Moghazi, A.M., Hassanen, M.A. 2000. Geochemistry, petrogenesis and tectonic setting of late Neoproterozoic Dokhan-type volcanic rocks in the Fatira area, Eastern Desert, Egypt. International Journal of Earth Sciences: 88, 764–777.

Moghazi, A.M. 1994. Geochemical and radiogenic isotope studies of some basement rocks at the Kid area, southeastern Sinai, Egypt. Unpublished Ph. D. Thesis, Alexandria University, Egypt, 377p.

Pearce, J.A. 1983. The role of subcontinental lithosphere in magma genesis at destructive plate margins, in: Hawkesworth, C.J., Norry, H.J. (Eds), Continental basalt and mantle xenoliths. Nantwich Shiva, pp. 230–249.

Pearce, J. A. 1996. Sources and settings of granitic rocks. Episode: 9, 120–125.

Pearce, J. A., Gale, G. H. 1977. Identification of ore-depositional environment from trace-element geochemistry of associated igneous host rocks. In: Volcanic processes in ore genesis. 7, Special Pubblication, Geological Society of London: 14–24.

Pearce, J.A., Norry, M.J. 1979. Petrogenetic implications of Ti, Zr, Y, and Nb variation in volcanic rocks. Contributions to Mineralogy and Petrology: 69, 33–47.

Pearce, J.A., Harris, N.B.W., Tindle, A.G. 1984. Trace element discrimination diagrams for the tectonic interpretation of granitic rocks. Journal of Petrology: 25, 956–983.

Peccerillo, A., Taylor, S.R. 1976. Geochemistry of Eocene calc-alkaline volcanic rocks from the Kastamonu area, northern Turkey. Contributions to Mineralogy and Petrology:58, 63–81.

Perrin, M., Saleh, A., Alva-Valdivia, L. 2009. Cenozoic and Mesozoic basalts from Egypt: a preliminary survey with a view to paleointensity. Earth, Planets and Space: 61, 51–60.

Ragab, A.I. 1987. On the petrogenesis of the DokhanVolcanics of the Northern Eastern Desert, Egypt. MERC Ain Shams University, Egypt: Earth Sciences Series: 1, 151–158.

Ressetar, R., Monrad, J.R. 1983. Chemical composition and tectonic setting of the DokhanVolcanics formation, Eastern Desert, Egypt. Journal of African Earth Sciences: 1, 103–112.

Segev, A. 1987. The age of the latest Precambrian volcanism in southern Israel, northeastern Sinai and SW Jordan: A re-

evaluation. Precambrian Research: 36, 277–285.

Solman, L.E. 1989. Triassic shoshonites from the Dolomites northern Italy: alkaline arc rocks in a strike-slip setting. Journal of Geophysical Research: 94, 4655–4666.

Stern, R. J. 1985. The Najd-fault system. Saudi Arabia and Egypt: A late Precambrian rift-related transform system?. Tectonics: 4, 497–511.

Stern, R.J. 1994. Arc assembly and continental collision in the Neoproterozoic East African Orogen: implications for the consolidation of Gondwanaland. Annual Reviews of Earth and Planetary Sciences: 22, 319–351.

Stern R.J., Gottfried, D., Hedge C.E. 1984. Late Precambrian rifting and crustal evolution in the northeast Desert of Egypt. Geology: 12: 168–172.

Stern, R.J., Hedge, C.E. 1985. Geochronological and isotopic constraints on Late-Precambrian crustal evolution in the Eastern Desert of Egypt. American Journal of Science: 285, 97–127.

Stern, R.J., Manton, W.I. 1987. Age of Feiran basement rocks, Sinai: implications for late Precambrian crustal evolution in the northern Arabian-Nubian Shield. Journal of the Geological Society of London: 144, 569–575.

Stern, R.J., Voegeli, D. A. 1987. Geochemistry, geochronology, and petrogenesis of a late Precambrian (=590 Ma) composite dyke from the north Eastern Desert of Egypt. Geologische Rundschau: 76, 325–341.

Stern, R.J., Sellers, G., Gottfried, D. 1988. Bimodal dyke swarms in the North Eastern Desert of Egypt: Significance for the origin of the late Precambrian "A-type" granites in northern Afro-Arabia, in: El-Gaby, S.A., Greiling, R.O. (Eds.), The Pan-African belt of northeast Africa and adjacent areas. Vieweg und Sohn, Weisbaden, Germany, pp. 147–177.

Sun, M. D., Chen, H. L., Zhang, F. Q., Wilde, S., Dong, C. W., Yang, S.F. 2013. A 100 Ma bimodal composite dyke complex in the Jianusi Block, NE China: an indication for lithospheric extension driven by Paleo-Pacific roll-back. Lithos: 162–163, 317–330.

Thompson, R.N., Morrison, M.A., Hendry, G.L., Parry, S.J. 1984. An assessment of the relative roles of crust and mantle in magma genesis: an elemental approach. Philosophical Transactions of the Royal Society of London: A 310, 549–590.

Wassif, N. A. 1991. Paleomagnetism and opaque mineral oxides of some basalt from west central Sinai, Egypt. Geophysical Journal International: 104, 319–330.

Wilde, S. A., Youssef, K. 2000. Significance of SHRIMP U-Pb dating of the Imperial Porphyry and associated DokhanVolcanics, Gebel Dokhan, north Eastern Desert, Egypt. Journal of African Earth Sciences: 31, 2, 403–413.

Wilde, S. A., Youssef, K. 2002. A re-evaluation of the origin and setting of the Late Precambrian Hammamat Group based on SHRIMP U-Pb dating of detrital zircons from Gebel Umm Tawat, North Eastern Desert, Egypt. Journal of Geological Society of London: 159, 595–604.

Winchester, J.A., Floyd, P.A. 1977. Geochemical discrimination of different magma series and their different products using immobile elements. Chemical Geology: 20, 325–343.